Tellus (2008), 60A, 1064–1078

TELLUS

Subjective versus objective sensitivity estimates: application to a North African cyclogenesis

By VICTOR HOMAR[1*] and DAVID J. STENSRUD[2], [1]*Edif. Mateu Orfila, Universitat de les Illes Balears. Palma de Mallorca, E-07122, Spain;* [2]*NOAA/National Severe Storms Laboratory, Norman, OK, USA*

(Manuscript received 18 July 2007; in final form 1 July 2008)

ABSTRACT

An observing system simulation experiment is used to test and compare objective and subjective estimates of sensitivity of a forecast aspect to the initial condition (IC) fields for a case of rapidly developing cyclogenesis over the Western Mediterranean during 19–22 December 1979. The ability of sensitivity estimation methods to provide helpful guidance about where an improvement in the IC can lead to the largest forecast error reduction is particularly important to ascertain in order to guide adaptive observation campaigns.

Synthetic soundings from a 15-km reference simulation are added to an initially poor 60-km control simulation over the sensitive areas as determined by the combination of the given sensitivity estimate and a simple analysis error estimate. The ability of each sensitivity estimation method to produce an improved simulation of the cyclone is assessed.

Results show that while the sensitivity estimates perform similarly, with no significant differences among them, the subjective method yields the best overall targeting guidance. In contrast, the adjoint estimate provides the least accurate targeting guidance for this particular case and analysis error estimate. This suggests that subjective sensitivity estimation methods are able to compete with or even improve upon the objective estimation method for this case of cyclogenesis over the Western Mediterranean.

1. Introduction

The initiatization of numerical weather prediction models has become a subject of increasing attention in recent years. The continuous improvement of model numerics, physical process parameterization schemes, and the continued improvements in computational resources have allowed operational models to be run at grid spacings below 10 km. Yet studies suggest that a detailed and accurate representation of the atmosphere is crucial for a successful forecast at subsynoptic scales (Stensrud and Fritsch, 1994), presenting a significant challenge for both data assimilation and observation strategies. The persistence of analysis errors in model initial conditions (ICs, Fritsch et al., 2000) has led to the development of several approaches to mitigate the effects of these errors in the forecast process. Emanuel et al. (1995) illustrate the utility of adaptive observations to reduce the analysis error over data-sensitive regions. Likewise, ensemble prediction systems based on IC perturbations recognize the presence of errors in the analyses and seek to include these uncertainties and their growth throughout the simulation period as a method to assess forecast confidence (Toth and Kalnay, 1997; Gelaro et al., 1998).

Both adaptive observing systems and perturbed IC ensemble strategies are based on the concept of IC error growth. In a pragmatic sense, only IC errors that grow during the simulation need to be considered when attempting to improve a forecast. Thus, an 'effective IC error' (F) must include two aspects: the analysis error (E) and the sensitivity (S) of a specified forecast aspect to the IC, such that $F_i = f(E, S)$ for each grid point i of the domain. The function f can conceivably have a very complex form. Regions with large F originate either from large analysis errors and appreciable sensitivity, appreciable analysis errors and large sensitivities, or moderate analysis errors and moderate sensitivities. In contrast, low values of effective error over an area indicate that either the analysis is relatively accurate or the sensitivity of the forecast over that area is negligible, or both, so that if large analysis errors exist, these errors do not 'effectively' degrade the forecast aspect of interest. In this study, we use the simplest possible form of f that fits these criteria, namely

$$F_i = E_i\ S_i. \tag{1}$$

When put in these simple terms, adaptive observation strategies and current IC ensemble prediction systems act to identify regions in the IC with large values of F and then either decrease

*Corresponding author.
e-mail: victor.homar@uib.es
DOI: 10.1111/j.1600-0870.2008.00353.x

E using adaptive observation strategies or account for the analysis errors by generating IC perturbations based on *F* that grow the fastest using ensemble prediction systems. We focus here on the use of adaptive observation strategies to decrease *E*.

Unfortunately, in real cases both the sensitivity field *S* and the analysis error *E* are unknown and so estimates of *S* and *E* are used to derive the 'effective error' (*F*). While many different approaches can be used to set bounds on the analysis error (e.g. Daley, 1991), we use a very simple form of *E* that is based on the operational sounding network density and investigate the differences found when using several estimates of the sensitivity *S* defined by objective and subjective sensitivity estimation methods. Adaptive observation techniques that account for the effects of the data assimilation system that assimilates the targeted observations are not evaluated.

In this study, we compare the skill of an adjoint model in a simulated adaptive observing system over the Mediterranean against several traditional subjective sensitivity estimates. The comparisons are carried out on a case of rapid cyclogenesis for an African low over the Western Mediterranean that occurred in December 1979. This allows for the comparison of the relatively complex and computationally expensive adjoint method against other less computationally expensive approaches and assess the often hypothesized better skill of the adjoint model for sensitivity estimates. This study also represents an initial exploratory step towards the development of targeting strategies for damaging weather situations in the Western Mediterranean. This is a basic objective of the MEDiterranean EXperiment on cyclones that produce high impact weather (MEDEX) and was also a part of the operations plan of the European THORPEX Regional Campaign 2007 (ETReC).

In order to assess the ability of the sensitivity estimates to identify regions in the IC where additional observations most effectively decrease the forecast error, an observing system simulation experiment is performed. Synthetic rawinsonde observations (soundings) are created from a 15-km reference simulation of the African low and assimilated into an initially deficient 60-km simulation of the same event started 12 h later. The decision about where the simulated observations are inserted is based on the sensitivity estimates and the assumed distribution of analysis error. The ability of the sensitivity estimates to provide good targeting guidance is assessed by analysing and comparing the resulting targeted simulations with the 15-km simulation of the cyclone.

The paper begins with a brief review of the sensitivity calculation and adaptive observations problems. A description of the model configuration used is detailed in Section 3. Section 4 presents a synoptic overview of the event and the poor-quality control run forecast. The set of sensitivity estimates used for this case are presented in Section 5. Section 6 discusses the details of the simulated observing system simulation experiment and the creation of simulated soundings. The results of the simulations and comparisons of the skill of each sensitivity estimate in reducing the forecast error is shown in Section 7. Discussion and final remarks are found in Section 8.

2. Background

The sensitivity of a given numerical forecast aspect, such as cyclone central pressure at a given time, can be estimated using a variety of approaches. Traditional sensitivity estimation is aimed at establishing cause-effect links and involves the diagnosis of an event followed by the subjective identification of potentially important structures in the IC. The method is usually based on conceptual models and straightforward Lagrangian back tracking of features through time (Lord, 1996; Ramis et al., 1998). These sensitivities often are verified by examining the effect of appropriate IC perturbations on the forecast. Extensions to this technique allow one to isolate the non-linear synergisms between IC perturbations by combining various perturbed experiments (Stein and Alpert, 1993). The traditional approach results in a qualitative estimation of the sensitivity, and is widely used to provide guidance in supplementary observational campaigns (Burpee et al., 1984; Lord, 1996) and attribution sensitivity studies (e.g. Romero, 2001).

The introduction of tangent linear and adjoint models into the numerical weather prediction community allows the computation of more objective sensitivity estimates for a given forecast aspect (Errico, 1997) at the expense of being restricted to the linear framework. Adjoint models have been used in adaptive observation campaigns such as the Fronts and Atlantic Storm-Track Experiment (FASTEX), the North Pacific Experiment (NORPEX, e.g. Langland et al., 1999a,b) and the 2003 Atlantic THORPEX Regional Campaign (ATReC, e.g. Truscott and Richardson, 2003), and they are also used operationally to compute singular vectors in the medium-range ensemble prediction system at the European Centre for Medium-range Weather Forecast (ECMWF, Gelaro et al., 1998). Adjoint models track the gradient of a forecast aspect with respect to the model state vector backward in time to determine its sensitivity to the IC state vector. To do so, a linear operator is constructed tangent to the phase space trajectory followed by the non-linear simulation. The transposition of such a linear operator results in the adjoint model. However, there are a number of theoretical and practical factors that hamper the accuracy of the adjoint-derived sensitivity (Errico, 1997). In addition to the intrinsic approximation due to the model tangent linearization, the linearization of diabatic processes is particularly complex and inaccurate. Moist processes and convective parameterization schemes involve a substantial number of non-differentiable operations, called on-off switches (Bao and Kuo, 1995; Xu, 1996), that limit the accuracy of the tangent linear and adjoint model results (Park and Droegemeier, 1997; Errico and Raeder, 1999). These limitations become even more important at the subsynoptic scale, where diabatic processes and convection govern an important fraction of the energy spectrum.

Adaptive observation strategies largely have been investigated only during the last decade. Real-time applications such as in the FASTEX, NORPEX, Winter Storm Reconnaissance and ATReC 2003 Programs have produced mixed results regarding the impact of targeted observations on mid-latitude winter cyclones forecasts (Gelaro et al., 1999; Langland et al., 1999a; Szunyogh et al., 1999; Toth et al., 2002; Weissmann et al., 2005). Lately, the assimilation scheme has been taken into account in the targeting decision-making process, yielding the sensitivity to observations rather than to the model IC (Baker and Daley, 2000; Doerenbecher and Bergot, 2001; Langland and Baker, 2004), although no direct guidance regarding unobserved areas is obtained. The calculation of sensitivities to observations offers an elegant framework to estimate, within the linear regime, the impact of an observation on the forecast aspect of interest while also accounting for the effects of the assimilation scheme. These methods do not directly provide guidance about where the targeted observations should be deployed, instead providing estimates of forecast performance given a set of proposed observations. In this way, a variety of proposed observational deployments can be analysed and the one that yields the most improved forecast can be determined. These methods explicitly account for the regional covariances used within the data assimilation system that might reveal influential observations located far from the regions with large adjoint IC sensitivity. Berliner et al. (1999) approaches this problem from a statistical design viewpoint and shows that optimal sites for targeted observations should be in locations with larger error and that are correlated with other unobserved sensitive regions.

An additional family of sensitivity estimation and targeting techniques have emerged from the proliferation and wide-spread availability of ensemble forecasts. Bishop et al. (2001) introduced the Ensemble Transform Kalman Filter (ETKF) technique that estimates potential numerical forecast error reductions by combining information on perturbation evolution with error statistics from an ensemble-based data assimilation scheme. Majumdar et al. (2006) and Reynolds et al. (2007) study in detail the differences between ETKF and adjoint-based methods for tropical and mid-latitude North-Atlantic cyclones, discussing the small differences in performance despite the notably different sensitivity estimates (analysis error driven and dynamically driven, respectively) that each method tends to produce. Another ensemble approach was first explored by Hakim and Torn (2008) who estimate forecast sensitivity by means of the linear relationship between IC perturbations and forecast perturbations in an ensemble forecasting system. Ancell and Hakim (2007a) analyse the differences between adjoint and ensemble-based sensitivity estimates for a sea level pressure 24-h forecast at a single point in the Pacific Northwest region of the United States. They show that ensemble sensitivities produce larger scale patterns and larger values of sensitivity owing to the statistical and dynamical character of each technique.

For the moment, no robust and efficient targeting strategy has been proposed and results vary largely from great forecast enhancements to strong degradations. Using a simplified model and idealized observations, Morss et al. (2001) and Morss and Emanuel (2002) describe the limitations of targeting systems and provide several scenarios where, even using a perfect model and perfect observations, adding observations in targeted areas degrade the forecast due to the inherent statistical and non-linear character of the data assimilation and forecast systems.

Here, a simple testbed for an adjoint-derived sensitivity estimate within an observation targeting experiment is carried out, analysing its accuracy against other simple methods to estimate IC sensitivity.

3. Basic numerical configuration

For all simulations presented in this study we use the Pennsylvania State University-National Center for Atmospheric Research (Penn State-NCAR) non-hydrostatic mesoscale modelling system version 5.3.6 (MM5, Grell et al., 1994; Dudhia et al., 2002). A single grid of 71×71 points at 60 km grid spacing, which covers all the Western Mediterranean, north Africa, the northwest Atlantic Ocean and Europe, is used (Fig. 1). In the vertical, 23 σ-levels with higher density at low levels are used. The forecast period extends to 60 h with a timestep of 180 s. The 60 h forecast length is selected because rapidly developing cyclones over the western Mediterranean can produce significant damage and an accurate 60 h forecast would provide the advance warning needed for disaster response preparation.

The standard MM5 includes many different options for the various physical parameterization schemes. For the present study, the Kain and Fritsch (1993) convective parameterization scheme, which includes shallow convection (Kain, 2002) is used. The resolved-scale moist processes follow the microphysics scheme of Reisner et al. (1998), which allows for cloud water, rain water, supercooled liquid water, cloud ice and snow. The planetary boundary layer is parameterized using the Hong and Pan (1996) scheme. Sea surface temperatures remain constant during the simulation and are taken from the National Centers for Environmental Prediction (NCEP) weekly analysis. A simple radiative cooling scheme is selected, which accounts for long- and short-wave interactions with clouds and clear air (Benjamin, 1983). Initial and boundary conditions are created using the three-dimensional variational (3DVAR) data assimilation system for the MM5 (Barker et al., 2004). The 3DVAR scheme combines a first-guess background state with observations to create an optimal analysis based on their statistical properties. The first-guess state is interpolated from the NCEP global $2.5^\circ \times 2.5^\circ$ analysis fields, and standard surface and upper-air observations are also provided to the variational analysis system. The observation errors are assumed to be spatially uncorrelated and a fixed, flow independent, background error matrix is used.

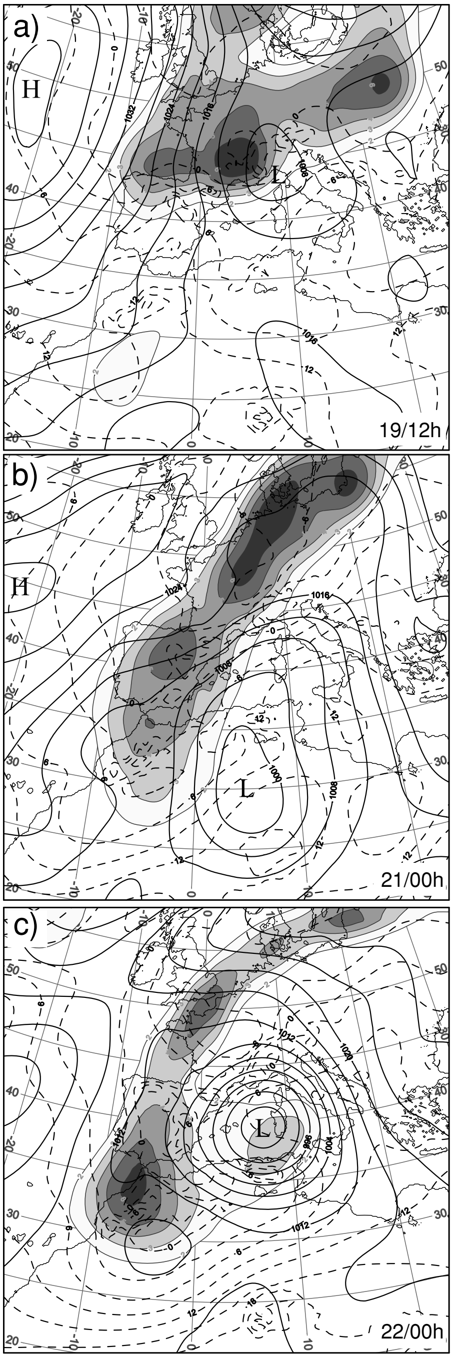

Fig. 1. 3DVAR analysis fields of 300 hPa PV (PVU, shaded), 900 hPa temperature (°C, dashed) and sea level pressure (hPa, solid) at (a) 12 UTC 19, (b) 00 UTC 21 and (c) 00 UTC 22 December 1979.

Time-dependent boundary conditions are supplied to the simulation by means of a relaxation inflow/outflow 5-point sponge frame based upon analyses from the 3DVAR system at 12 h intervals. An upper radiative condition is used to minimize spurious noise reflection at the model top.

4. Synoptic overview

The case used for this study is a rapidly developing cyclone over the Western Mediterranean that occurred from 19 to 22 December 1979. Homar et al. (2002) present a detailed numerical analysis of the event, highlighting an initial stage of strong baroclinically forced deepening over north Africa followed by a period of intense latent heat release from convection when the cyclone core reaches the warm western Mediterranean Sea. The analysed pressure drop at the centre of the cyclone during the 24 h period starting 00 UTC 21 December fulfils the Sanders and Gyakum (1980) condition for rapidly deepening cyclones (0.7 hPa h^{-1} during 24 h at 40 °N). Sustained winds over land of 10 ms^{-1} and gusts exceeding 30 ms^{-1} are reported over periods exceeding more than 78 h at some stations on the Balearic Islands.

The event begins with a broad surface high sitting over the northwestern Atlantic which, together with a dissipating depression over the northern portion of the Western Mediterranean, produce northerly cold advection over the Iberian Peninsula and northwestern Africa (Fig. 1a). At the upper levels, a wide cold trough covers most of Europe, with three secondary waves visible as relative maxima on the 300 hPa potential vorticity (PV) field. Over the next 36 h, the westernmost PV maximum extends farther to the southwest and then it begins to roll-up northeastwards, while at low levels an extensive cyclone develops over North Africa linked to the low-level frontal zone (Fig. 1b). Over the following 24 h, the cyclone intensifies and moves northward toward the Mediterranean Sea. By 00 UTC 22 December, a deep and round cyclone covers the Western Mediterranean with strong winds affecting northern Italy, southern France and eastern Spain (Fig. 1c). At this time, the minimum central pressure computed by the analysis over the sea is 982 hPa and located to the east of the Balearic Islands.

4.1. Control run

Using the numerical set-up detailed in Section 3, we run a 60 h simulation starting at 12 UTC 19 December 1979. This experiment does not reproduce the intensity or shape of the analysed cyclone. The simulated cyclone has a central pressure of only 999 hPa (17 hPa above the analysis) and an elongated north-south shape with less intense sea level pressure gradients than indicated by the analysis (Fig. 2). As seen on the PV field, these discrepancies are likely related to the inability of the model to reproduce accurately the detailed evolution of the upper-level shortwave trough. In particular, the eastern PV anomaly analysed directly over the surface cyclone centre (Fig. 1c) is not an isolated nuclei in the simulation but a wide eastward extension of the main PV streamer. This results in weaker but more widespread cyclogenetic forcing from the upper trough and a less localized low.

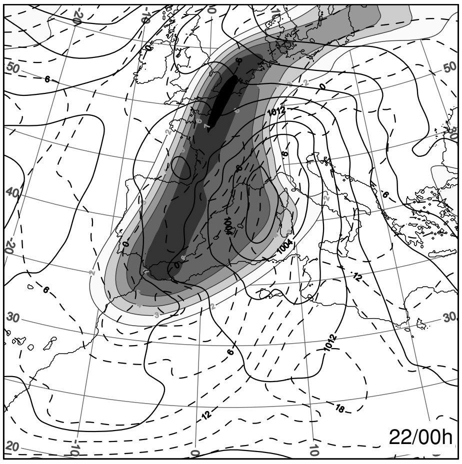

Fig. 2. As in Fig. 1, but for the 60-km control run: 60 h forecast valid at 00 UTC 22 December.

This simulation is used as the control run due to its a priori significant potential for forecast improvement with respect to the cyclone intensity and shape at 00 UTC 22 December. Accurate forecasts of these Western Mediterranean cyclones and the interaction of their associated winds with the topographic ranges of the region are of primary importance to predicting episodes of heavy rainfall and damaging winds over the populated coastal areas of the Mediterranean basin. Indeed, the THORPEX–MEDEX project is founded on this fundamental hypothesis.

5. Sensitivity estimates

The ability of various sensitivity estimation techniques to identify the structures in the 12 UTC 19 December fields (Fig. 1a) that are important to the development of the intense Mediterranean cyclone observed at 00 UTC 22 December are now explored (Fig. 1c). Although numerous methods have been used to directly or indirectly estimate the most influential areas for the prediction of an aspect of interest in a numerical forecast, we focus our attention on two groups of methods: 'objective' and 'subjective'. We define 'objective' methods as those based on the tangent linear and adjoint models. Other objective sensitivity estimation methods such as the ensemble transform Kalman technique (Bishop et al., 2001) or tangent linear inverse methods (Pu et al., 1997) are not considered. We define 'subjective' methods as those based on the human interpretation of the atmospheric fields and the use of links between the chosen forecast aspect and the IC structures as derived from conceptual models. We recognize that the chosen sensitivity estimation methods do not represent an exhaustive list of all adaptive observation strategies, but believe that the results presented herein are worth consideration in targeting campaigns planning to use targeting strategies similar to those presented here.

5.1. Adjoint estimate

We use the MM5 adjoint model (Zou et al., 1997, 1998) to compute the sensitivity of this intense Mediterranean cyclone simulation to the IC fields. For this run, we use the same grid and time span as for the control run. Although this maritime cyclogenesis event has important contributions from convective heating during the second stage of cyclone deepening, we do not use the convective parameterization available in the adjoint due to inconsistencies in the linearization of the convective scheme as shown by Homar and Stensrud (2004). However, the adjoint of the Dudhia (1989) microphysics scheme is included in the model to account for grid-scale microphysical processes. A simple bulk boundary layer parameterization is used. In order to run a tangent linear simulation, the basic state non-linear trajectory needs to be stored. We use an every-timestep update to avoid any degradation from this source in the results (Errico et al., 1993). Using this configuration, we define a response function of interest and the adjoint model traces back its sensitivity, computing the gradients of the response function with respect to the model state.

It is well known that sensitivity fields computed by the adjoint are very dependent upon the definition of the response function. We define the response function as the pressure at the lowest model level over the predicted cyclone centre at 00 UTC 22 December. Other relevant characteristics of the cyclone, such as the winds close to the core, are not included explicitly in this response function. While the adjoint does not strictly guarantee that these other variables are affected, we expect that producing a deeper cyclone will yield improvements to the predicted cyclone's shape and associated winds. The adjoint computes the gradients of the response function to perturbations in the fields at the 12 UTC 19 December model start time.

Regarding the validity of the adjoint model or its ability to compute accurate sensitivity fields for this case, no strict test of the linear approximation is performed for this simulation. However, the combination of the initial synoptic-scale baroclinic development of the cyclone (that is likely to have a large linear component) followed by an intensification stage forced by mesoscale processes (that are likely to have a larger non-linear component and thus hamper the adjoint results) provides a good opportunity to use the adjoint estimation method in comparison with subjective sensitivity estimates for this important type of rapidly developing cyclone. The strict assessment of the tangent-linear range to IC perturbation amplitudes, as presented in Homar and Stensrud (2004), is too demanding to be implemented in real-time targeting campaigns, suggesting that the experimental setup used here is realistic. We recognize, however, that non-linear effects become important by 48 h (Gilmour et al., 2001), likely placing a bound on the forecast improvements expected.

In order to summarize the three-dimensional sensitivity estimates, vertical and horizontal averages of the absolute values of the adjoint variables $\hat{u}$, $\hat{v}$ [hPa (ms^{-1})$^{-1}$], $\hat{T}$ (hPa K^{-1}), $\hat{p}$

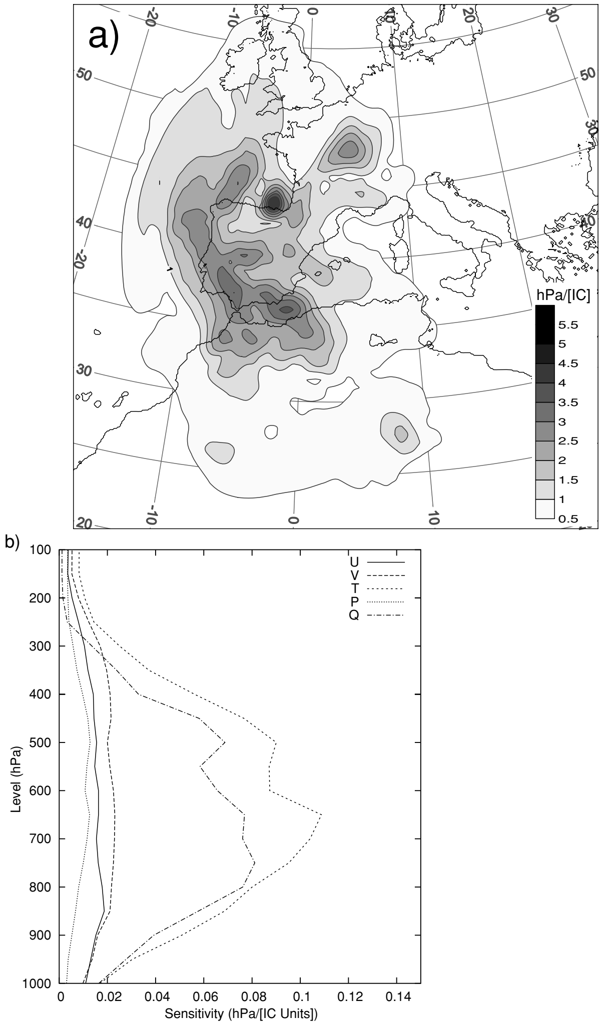

Fig. 3. Adjoint model results. (a) Vertical average of the absolute value of the sensitivities of u, v, T, p and q (units are non-physical hPa/[Model Input]). (b) Vertical distribution of the horizontal (pressure level) average of the individual sensitivities {corresponding units are hPa/[(m s^{-1}), K, hPa, g kg^{-1}]} versus pressure.

(hPa hPa^{-1}) and $\hat{q}$ [hPa (g kg^{-1})$^{-1}$] are computed. While this field is inherently ill-defined because the averaged fields have different units, it is a convenient index that provides a concise visualization of the sensitivity distribution across the domain. The sensitivity results focus primarily on the western and southern parts of the Iberian Peninsula (Fig. 3a), though significant sensitivity extends westward over the Atlantic toward the British Isles and over north Africa. Temperature and specific humidity show the largest sensitivities, with maximum amplitudes at mid- to low levels (Fig. 3b). This vertical distribution and the dominance of the temperature and specific humidity variables is characteristic of adjoint results for cyclogenesis events as described by Langland et al. (1995), Lewis et al. (2001) and Homar and Stensrud (2004). An analysis and interpretation of the large sensitivities found in the mid- and low levels, as opposed to sensitivities in upper tropospheric structures, for short range (24–72 h) forecasts is provided by Gelaro et al. (2000) and Badger and Hoskins (2001). The two-dimensional synopsis of the adjoint results shown in Fig. 3a is used as the sensitivity S needed to compute the effective error F in eq. (1).

Although more complex measures of the analysis error E can be computed from data assimilation systems, we choose a simple estimate computed as a function of the sounding network density, in which

$$E(x, y) = \prod_{\text{Stations}} \left[1 - e^{-\frac{(x_s - x)^2 + (y_s - y)^2}{\sigma^2}} \right], \qquad (2)$$

where x_s and y_s correspond to the sounding locations, and σ is the standard deviation that defines the area of influence of each station. Thus, we assume that each station reduces the analysis error following a two-dimensional Gaussian function around the sounding location. Although in a rigorous sense the effect of each sounding extends over the whole domain in variational assimilation systems, inspection of the typical local perturbation induced by several test soundings on the 3DVAR analysis fields suggests a σ value of 600 km for this particular case.

The effective error F is computed by multiplying the sensitivity S (Fig. 3a) with the error estimate E (eq. 2). Note that $E(x_s, y_s) = 0$ and so $F(x_s, y_s) = 0$ at each sounding location, and therefore no targeted observation is placed over a fixed sounding station. The resulting effective error (Fig. 4) highlights areas where the sounding density is low and the sensitivity of the forecast aspect is high, suggesting that an improvement of the

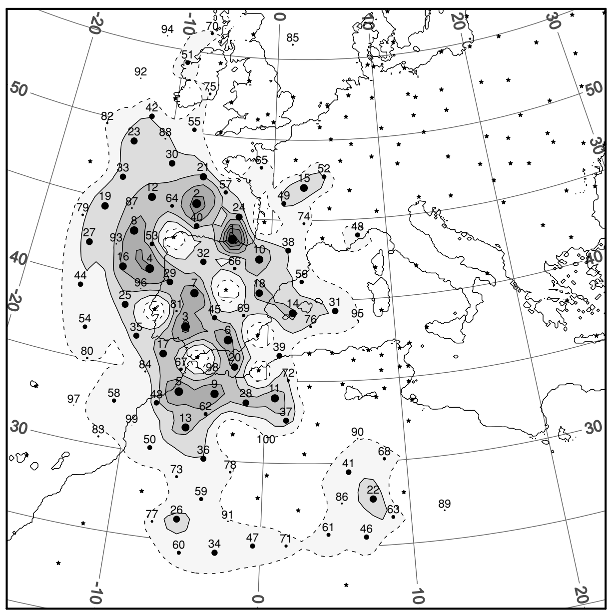

Fig. 4. Effective error F for the adjoint-derived sensitivity estimate. Available real sounding stations are indicated with stars. Black dots show the list of the 100 new targeted observations (in order).

analysis in these areas has a larger impact on the forecast error. The results show that despite the existence of a number of fixed stations over the Iberian peninsula, the effective error F suggests that a better sampling of the IC fields over this region would benefit the prediction more than improved sampling over many other regions in the domain that are less densely observed. On the other hand, over west Algeria, Tunisia, the British Isles and most of central Europe, the regular fixed sounding observations provide, as suggested by this adjoint-derived effective error, enough accuracy to the IC fields to not contribute significantly to the forecast error for the cyclone development.

5.2. *Gradients estimate*

This subjective sensitivity estimate is entirely based on a simple attribution of the sensitivity to structures in the IC that are likely to have a role in cyclogenetic development. Mid- to upper-level PV anomalies, low level baroclinic regions, jets-streaks and moisture boundaries are features which contribute to cyclogenesis and usually govern the generation of intense phenomena (e.g. Carlson, 1991). Thus, this estimate is defined as the vertical average of the normalized absolute value of the gradients of PV, temperature, wind speed and specific humidity. The aim of this approach is to place targeted observations where they better represent a priori important features in the IC to improve the forecast. The effective error F obtained from this estimate S and the analysis error E from eq. (2), shows that this method focuses on a good representation of the incipient secondary upper-level trough and associated jet-stream (Fig. 5) and on the north African environment where this upper-level system further evolves and the cyclogenesis occurs.

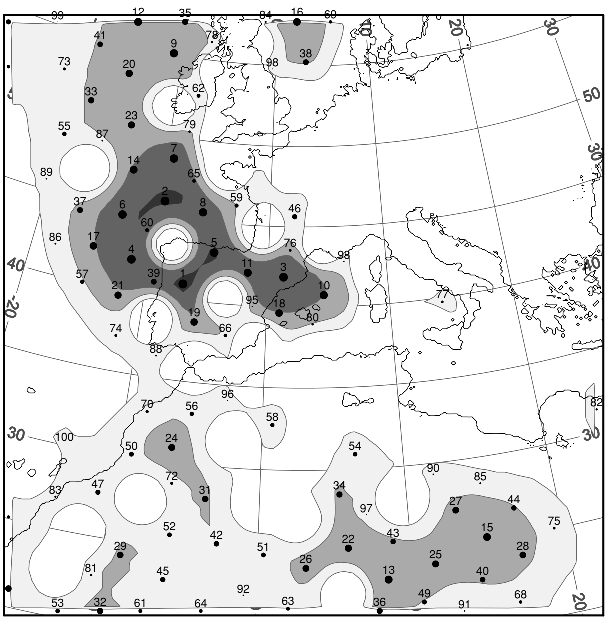

Fig. 5. Effective error F for the gradients sensitivity estimate (see text for details). Black dots show the rank list of the 100 new targeted observations (in order).

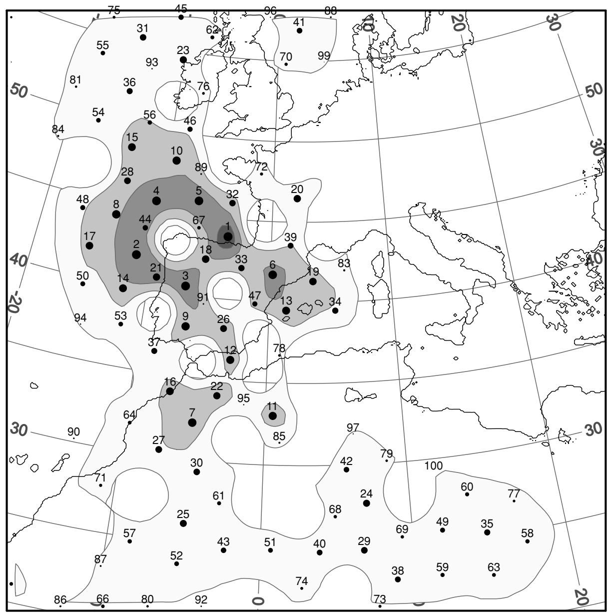

Fig. 6. As in Fig. 5 but for the combined estimates.

5.3. *Combined estimate*

The two sensitivity estimation methods that can be created automatically, the adjoint and gradient estimates, are combined by taking the mean of these two sensitivity estimates and multiplying by the assumed analysis error distribution. This approach admits that combining both methods may incorporate ingredients that are missed by either method but eventually influential in the full non-linear model. Thus, we evaluate whether or not the mean of these two sensitivity estimates (Fig. 6) can capture better the actual non-linear sensitivity and yield an improved simulation of the cyclone.

5.4. *Manual estimates*

Two manual subjective sensitivity estimates also are included in the comparisons, with each author producing one manual selection of targeting locations. For this test, the fields explicit sensitivity S and effective error E are not computed or used. Instead, the manual selection of the desired sounding observations is based upon a visual inspection of the IC fields, with particular attention paid to the upper-level PV structures, and knowledge of the fixed sounding station locations. This procedure mimics the traditional adaptive observational decision-making process, where a team of meteorologists decide where extra observations are convenient without the support from sensitivity fields. Two manual experiments are made to ascertain the robustness of this

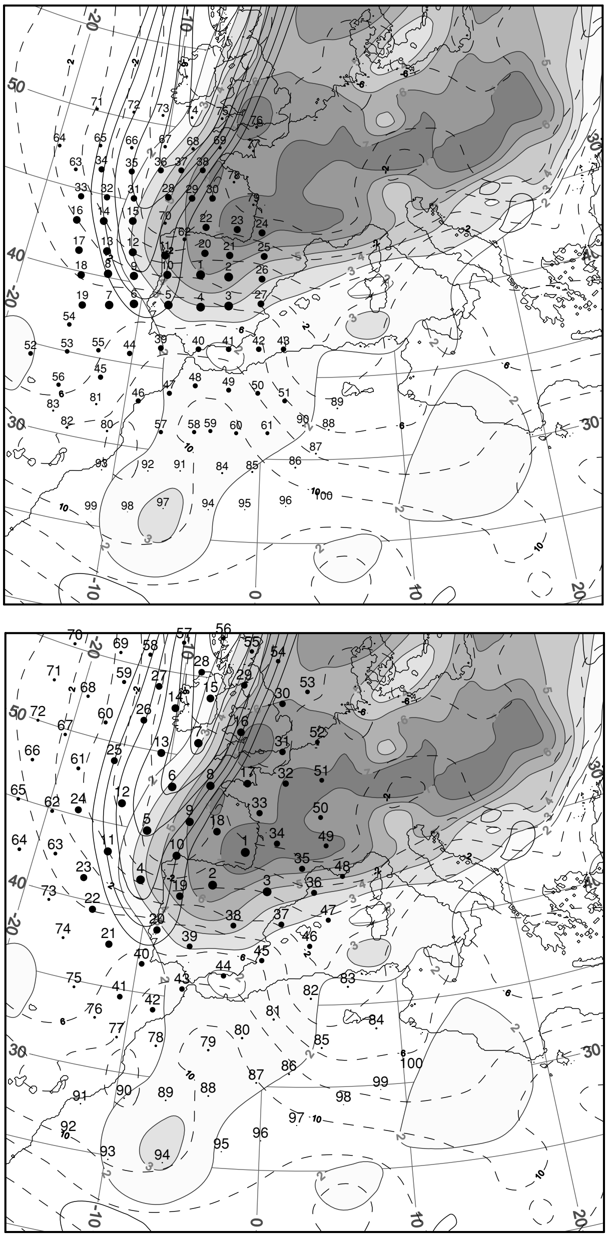

Fig. 7. Manual selection of location for targeted observations. The fields that are used to guide the selection, 3DVAR analysis at 12 UTC 19 December 1979, are plotted: PV at 250 hPa (PVU, shaded), temperature at 850 hPa (°C, dashed), and wind speed at 250 hPa (solid, $\Delta = 5 \geq 40$ ms^{-1}). Panels depict (a) Manual I and (b) Manual II selections referred to in the text.

approach and avoid the possible pathological characteristics of one single manual sample of stations. The selected stations and the main fields used to choose them are shown in Fig. 7. While one author is very familiar with this case and perhaps can use this knowledge to provide the best possible selection of soundings, the other author is not very familiar with this case. In general both selections of stations focus over the southern and south-western edges of a PV anomaly, the leading edge of the 250 hPa jet streak and the warm surge visible over the southern Iberian Peninsula and Morroco at 900 hPa. This is dynamically justified since the interaction of all three sampled agents is crucial for the posterior Mediterranean cyclogenesis (Homar et al., 2002). It is our hypothesis that if both manual sensitivity estimates perform well, similar results will be obtained in real adaptive observing campaigns led by experienced forecasters for the region.

6. Observing simulation system experiment (OSSE)

With the sensitivity estimates now defined, an OSSE is created to provide a simulated atmospheric state from which soundings are extracted. An identical set-up as the control run (Section 3) is used for this experiment, except that the grid spacing is increased up to 15 km (281 × 281 grid points and a 45 s timestep), the simulation starts 12 h prior to the control run (00 UTC 19 December), and the ECMWF re-analyses are used as the first-guess fields for the 3DVAR system. This simulation will play the role of synthetic ‘truth’ from where additional soundings for the targeted simulations will be extracted. The use of a higher resolution run from which to extract synthetic soundings adds realism to the OSSE framework as it naturally includes differences in representativeness between the forecast model at 60 km and the synthetic observations at 15 km; differences in representativeness between the forecast model and real sounding observations are even larger.

Results from this high resolution run are shown in Fig. 8. The forecast at the verification time (00 UTC 22 December) shows a sea level pressure minimum of 988 (7 hPa above the analysis and 11 hPa below the control run) and surface winds over the Balearics reaching 23 m s^{-1}. Linked to this more focused depression and rounder circulation about the cyclone centre, this simulation forecasts a well defined PV anomaly at the upper levels over the cyclone core.

The high resolution simulation is started at 00 UTC 19 December to allow the model to spin-up all resolvable scales prior to the 12 UTC 19 December start time of the 60 km control run. The targeting process consists of extracting soundings sequentially from the 12 h forecast fields of the high resolution simulation (Fig. 8a) at the locations of maximum effective error F (as shown in Figs. 4–7) and adding these simulated soundings to the 60 km control run 3DVAR data assimilation system. After each new station is added, a recalculation of E (eq. 2) is done and a new F is computed. Thus, the effective error fields change as new soundings are added to the simulation. The targeting framework is mimiced by using the fixed sensitivity estimates determined from the control run. For the case of Manual estimates, the soundings are extracted in the order presented in Fig. 7. By comparing the different resulting targeted simulations, the ability of each sensitivity estimation method to determine the

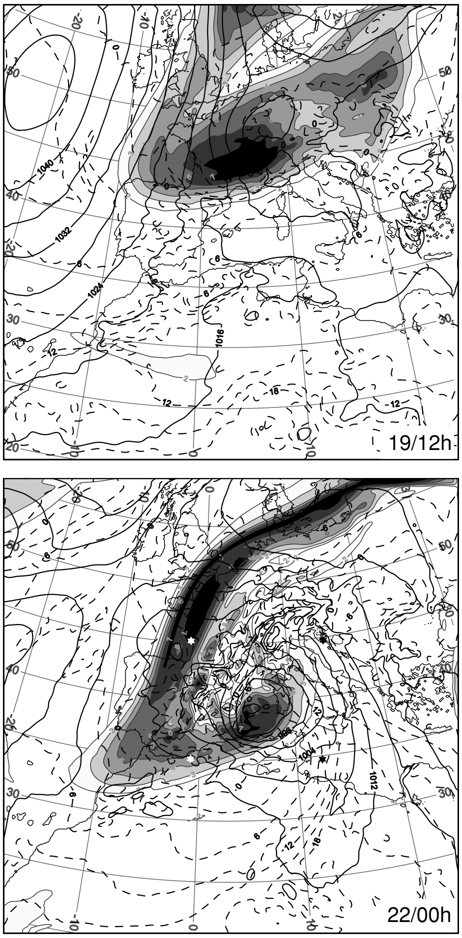

Fig. 8. Fields of sea level pressure (hPa, solid), temperature at 900 hPa (°C, dashed) and PV at 300 hPa (PVU, shaded) from OSSE 15-km simulation for upper panel: 12 UTC 19 December (initial time for control and targeted simulations) and lower panel: 00 UTC 22 December (verification time). Stars in panel (b) indicate the corners of the rectangular area used to compute PV correlations presented in Section 7.

areas where additional soundings yield an improved simulation is evaluated.

The simulated soundings are created from the 15 km OSSE simulation and supplied to the 60 km 3DVAR experiments together with the actual observations. The error statistics associated with the targeted soundings are the same as those used for the real soundings (i.e. constant and spatially uncorrelated).

7. Targeted simulations comparison

The simulated soundings are added to the actual observed soundings one by one and new ICs can be created by the 3DVAR scheme after each new sounding is added. Due to 3DVAR covariances, the analysis increments attributed to each additional sounding extend beyond a single grid point, thus not rigorously guaranteeing that the analysis error is reduced over a sensitive area (Langland and Baker, 2004). However, in practice, an observation most strongly influences its nearby surroundings, and in this study the estimation of the analysis error is done under this hypothesis (eq. 2). Examination of the analysis increments shows that no significant increments are found at distances longer than 500 km from the observation site. If we are to assimilate soundings one by one, for the first 100 stations from each of the five sensitivity estimates, this evaluation would require 500 new ICs and 500 runs. Thus, to reduce the computational cost, we limit the targeted simulations to 12 runs per experiment that occur after 1, 2, 3, 5, 10, 15, 20, 30, 40, 50, 75 and 100 new stations are added. More attention is focused upon the addition of the first groups of sounding observations to resolve better the ability of the sensitivity estimates to improve the simulation with a smaller number of observations. Current targeting campaigns typically use about 20 dropsondes per mission with horizontal spacings of 100–250 km (Langland et al., 1999a).

The first forecast aspect analysed is the cyclone central sea level pressure (SLP) value. However, the cyclone centre is not at the same location in all simulations. Focusing on the minimum pressure over a predefined area of interest, we allow for the effect of new observations to change not only the cyclone depth but also change it's position. Results indicate that the general tendency using all 100 stations is to produce a deeper cyclone (Fig. 9a), so that adding stations based upon any of the estimation methods is beneficial. This confirms the simple idea that for a large enough number of targeted stations in sensitive regions the forecast error is eventually reduced. However, all experiments show an initial filling of the cyclone as the first 5–10 stations are added, with most of the runs not showing central pressures below the original control run 998.5 hPa until more than 40 additional observations are added. The degrading effect of new observations also is detected in several episodes of real targeting campaigns (Szunyogh et al., 1999) and some of the causes are investigated by Morss et al. (2001) and Morss and Emanuel (2002). The most common interpretation for this problem, besides deficiencies in the sensitivity estimate, is the presence of significant representative errors, caused by an inadequate sampling of the important structures in the model IC. However, this interpretation is difficult to apply here since the two experiments with the densest network of stations in the sensitive area (i.e. Manual I and Adjoint) yield the best and worst simulations, respectively, for the simulated cyclone central pressure. Overall, large improvements in the prediction of cyclone central pressure are not seen for the targeted simulations. Except for the Manual I, the maximum reduction in cyclone central pressure for all the simulations is less than 2 hPa after adding 100 targeted soundings, which is only a small fraction of the initial 10 hPa error of the control run. Note that an alternative control simulation of this event using ECMWF initial fields with the same 60 km grid is able to yield a cyclone central pressure of 991 hPa (3 hPa above the OSSE run and

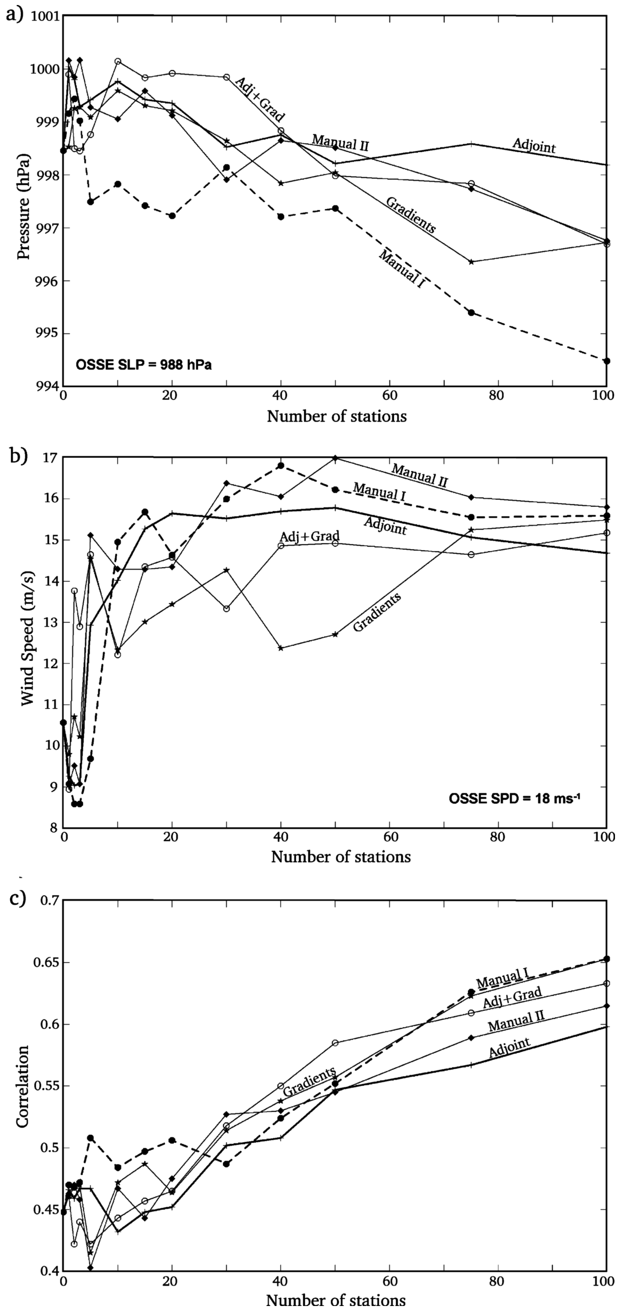

Fig. 9. Forecast aspects as a function of the number of targeted stations for (a) central SLP (hPa), (b) wind speed at 1000 hPa over the Balearic Islands (ms^{-1}) and (c) spatial correlation of PV at 300 hPa (PVU) against the OSSE 'truth' simulation over an area over the cyclone, as indicated in Fig. 8b.

4 hPa below Manual I), indicating that it is possible to produce a reasonably accurate simulation of this case at this resolution.

The wind speed prediction over the Balearic Islands shows a more substantial benefit from the new observations (Fig. 9b). Although these curves also show that the errors again increase as the first 1–5 soundings are added, all the simulations exhibit a rapid improvement of 4–5 m s^{-1} as the number of additional soundings reaches the range of 5–20. Unlike the relatively linear character of the cyclone central pressure curves, the wind speed response to the targeted observations is closer to an ideal response, where a large improvement occurs for the first few additional soundings and is followed by a more asymptotic error reduction as targeted soundings are added from locations farther from the main sensitivity area. Considering the very different sensitivity estimation methods used, the similarity of the responses in the resulting simulations to the additional soundings is remarkable. No significant differences exist, although the lowest errors are achieved by the two manual sensitivity estimates. The gradients estimate has the worst wind speed simulations over the Balearic Islands until 75–100 additional soundings are added.

To investigate the predictions of the main dynamical driver of the cyclogenesis, the upper-level PV simulations are compared to the OSSE run by computing the spatial correlation of the 300 hPa PV fields over an area covering the Western Mediterranean. The apparent link between the evolution of the upper-level trough and the shape and intensity of the forecast surface cyclone, and the failure of the control run to reproduce the isolated PV anomaly over the cyclone centre (see Figs 2 and 8b), suggests that PV also is an important field to evaluate. Again, the results show no overall significant differences between the experiments; all of them indicate a nearly linear increase in correlation with the number of soundings (Fig. 9c). As seen with the wind speed results, the accuracy of the upper-level fields improves consistently as new soundings are added. This nearly constant improvement suggests that all the soundings contribute almost equally to decreasing the forecast error. Several of the estimation methods (Manual, Gradients and Combined) add soundings far to the south and north of the main PV feature. This suggests that, to obtain a correct representation of the evolution of the upper level PV field, it is equally important to correctly sample the main incipient secondary trough, which later enlarges and intensifies, and the remote areas which interact with the trough during the event.

Although no dramatic differences exist between the simulations, the comparisons show a slight overall advantage of the Manual I and Gradient sensitivity estimates. The adjoint estimate provides only moderate improvements to the control simulation and yields the worst guidance for the cyclone deepening and the upper-level PV structure. The inability of the adjoint estimation method to improve the cyclone central pressure is an unexpected result: on one hand, the analysis increments due to additional soundings are well confined to the areas surrounding the targeted sites, thus modifying the IC fields only in adjoint-derived sensitive areas (not shown) and limiting the effects from distant analysis increments [such as those described by Ancell and Hakim (2007b)]; on the other hand, the cyclone central pressure is the parameter most closely related to the response function

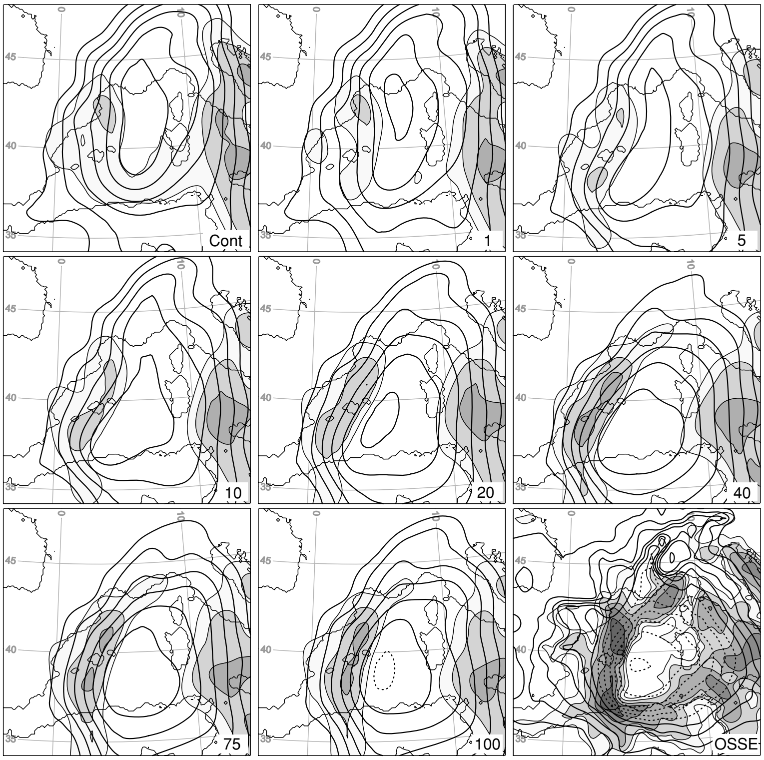

Fig. 10. Postage-stamp plots of SLP and wind speed at 1000 hPa for the series of targeted simulations using the adjoint sensitivity estimate. Lines show SLP $\leq$ 1010 hPa (dashed $\leq$ 998 hPa) with an interval of 2 hPa. Shaded field is wind speed $\geq$ 10 ms^{-1} at 1000 hPa with an interval of 3 ms^{-1}. Simulations with 2, 3, 15, 30 and 50 targeted observations are not shown for brevity. First panel shows the control run (0 observations) and last panel is the OSSE run.

defined in the adjoint model and so was expected to provide the best results. Temperature analysis increments exceeding 3 °C are found in adjoint-sensitive areas for targeted simulations, which were shown by Homar and Stensrud (2004) to bring the forecast model significantly away from the linear regime for a similar Mediterranean cyclogenetic case. Therefore, the linearity of the adjoint estimates is probably the main degrading cause for the adjoint-based results.

To better understand the differences between the central pressure and wind speed results, the evolution of these fields as new targeted soundings are added to the simulation is evaluated (Figs. 10 and 11). It may be that adaptive observation techniques that account for the effects of the data assimilation system that assimilates the targeted observations (e.g. Berliner et al., 1999; Langland and Baker, 2004) could yield better results. For the sake of brevity, only the fields for the Adjoint and Manual I simulations are shown as results from the other simulations are similar. Focusing first on the SLP pattern, clear differences in the two simulations emerge. The targeted soundings are intended to improve the location (toward the southwest), the shape (less eccentric) and the depth (11 hPa deeper) of the cyclone from the control run. The first soundings added in the Adjoint simulation produce a southern shift of the cyclone with almost no change in the shape and an increase of the central SLP. As between 25 and 75 additional soundings are added, the cyclone shape finally becomes more rounded, likely due to the more isolated character of the upper-level PV anomaly (not shown). In contrast, the evolution of the Manual I simulation shows a smoother relaxation toward the observed cyclone characteristics (Fig. 11). A distinct change in cyclone shape and location is seen as 5–10 soundings are added. While the simulated cyclone locations from the adjoint and manual simulations are not very different, an accurate cyclone location is needed to anticipate damaging weather in the region. In the Western Mediterranean, high topographic ranges are located close to the coast, so an accurate forecast of the position of the cyclone centre, and especially the direction and intensity of the associated circulation, are of primary concern when predicting heavy precipitation or damaging winds events (Jansà et al., 2001).

Differences in the structures of the low-level jet are not significant between these two simulations. Results indicate that as long as the cyclone is shifted to the southwest as additional targeted soundings are added, producing northeasterly flow near the Spanish coast, the winds between the cyclone and the eastern Iberian Peninsula coast are well simulated regardless of the absolute depth of the cyclone (Figs. 10 and 11). This close relationship between the low-level jet and the cyclone position, and not between the low-level jet and cyclone depth, explains the differences in simulation accuracy shown in Figs. 9a and b.

7.1. *Verification and stability tests*

In order to determine whether or not the sensitivity estimation methods target the most important features needed to improve

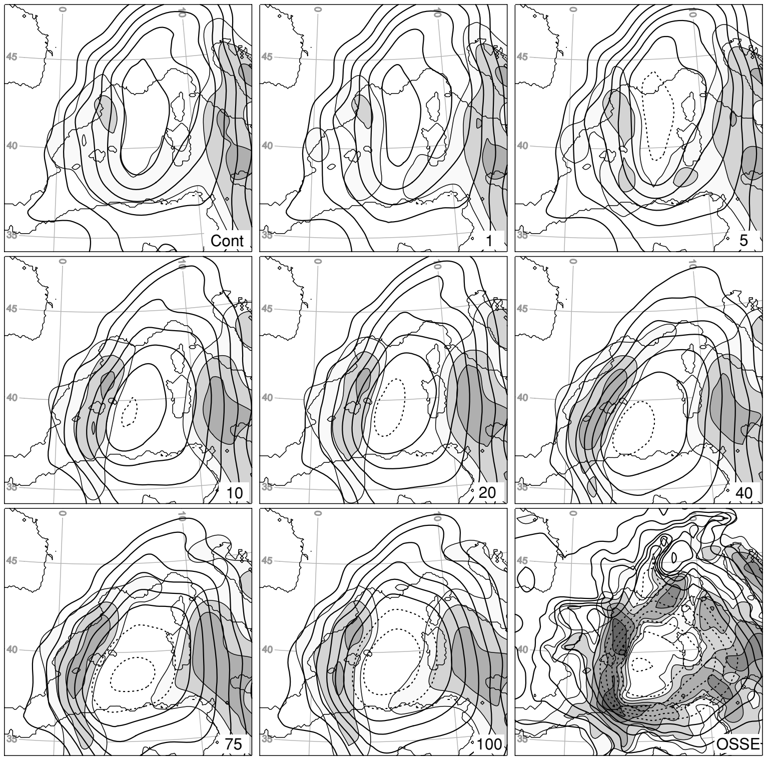

Fig. 11. As in Fig. 10 but for manual I sensitivity estimate.

the simulation of the cyclone, a 'null' experiment is designed in which the sounding locations are assimilated using an inverted criterion. Soundings in this experiment are selected from areas with the smallest effective error *F*. Results from these experiments (not shown) reveal very small differences from the control run. This confirms that the sensitivity estimates developed are able to identify at least the general areas of high and low sensitivity across the domain. In a more demanding test, and focusing on the adjoint method, another experiment is performed assimilating the 100 soundings whose location are determined by the adjoint sensitivity but inverting the order in which they are assimilated. Thus, the targeted soundings still are located over areas with appreciable sensitivity. Compared to the earlier adjoint sensitivity results, different responses are obtained for the three parameters analysed (Fig. 12). For the central SLP, the inverted series produces deeper cyclones than the original adjoint simulation for the first 30 additional soundings, although the overall tendency is more variable as the number of soundings is increased. The 300 hPa PV correlation shows a clear improvement when using the inverted series, with the largest

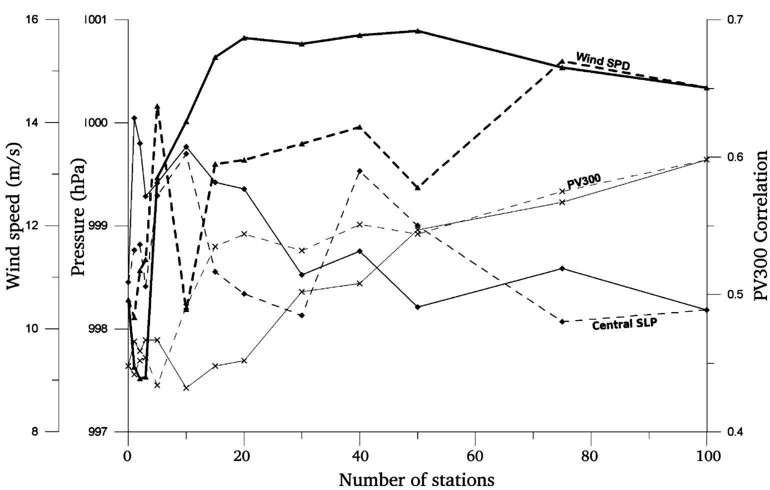

Fig. 12. Comparison between the original adjoint simulations (solid lines) and the inverted order experiment (dashed) for the central SLP (diamonds), wind speed over the Balearics (triangles) and upper-level PV pattern correlation (crosses).

change occurring as the first 10–20 soundings are added as expected from an ideal targeting strategy. On the other hand, the wind speed over the Balearics yields worse results than the original, with the improvement originally occurring after 10–20 new soundings delayed until after 30–50 new soundings are added in the inverted sequence.

These results raise some concerns about using an adjoint method to estimate sensitivity distribution for observation targeting. Although the adjoint sensitivities certainly give a general indication of the areas suitable for optimal targeting, in agreement with the subjective methods used, the information garnished about the particular locations of the new soundings may not be as reliable as one might desire in a targeting campaign.

The last aspect tested regarding the proposed targeting methods is the robustness of the results with respect to the location of the soundings. This test is carried out by replacing each original sounding in the data set by a randomly selected sounding from a neighbouring grid point. Thus, the soundings that are used in the 3DVAR system are from locations 15 km away from all the original soundings. The ratio between the variations in these perturbed simulations and the overall changes obtained by adding new soundings provides an indication of the representativity of the results in terms of the predictability of the forecast aspect under analysis. For the experiments performed in this study, these perturbed sounding location runs show consistent variations of about 40% of the typical forecast change due to the addition of new soundings. This shows that, despite the limited predictability of the phenomena at the 60 h simulation time, a better representation of the IC fields still improves the forecast. Therefore, the more accurate forecasts obtained for the targeted simulations are not the result of a lucky guess but are due to the identification of really sensitive structures in the model ICs.

8. Discussion and conclusions

The ability of both objective and subjective sensitivity estimation methods to estimate sensitivities in the ICs of a simulation of an intense cyclogenesis event over the Western Mediterranean is examined. Results from one objective sensitivity estimate, provided by an adjoint model and three subjective sensitivity estimates are compared and contrasted. An observation system simulation experiment is developed to provide a data source for simulated soundings that are sequentially assimilated in a 3DVAR system at locations determined by the sensitivity estimation methods. Simulations of the intense cyclogenesis event are undertaken after the targeted simulated soundings are assimilated and results from these simulations compared to provide guidance on which sensitivity estimation techniques yield the most realistic cyclone forecast. We have carried out this comparison by focusing on three forecast aspects related to the intensity of the simulated Mediterranean cyclone: central SLP, wind speed over the Balearic Islands, and the upper-level PV pattern over the cyclone.

Results indicate that all the methods yield comparable results and fail to capture the intense deepening of the cyclone. However, of the techniques evaluated and under the designed framework, the adjoint estimate is inferior to the other sensitivity estimates. The guidance offered by a simple depiction of the gradients of several standard fields in the model IC, such as the PV, wind speed, temperature and specific humidity, is equal to or better than the adjoint-derived sensitivities in our simulated targeting framework. Additionally, while a manual selection of targeted observations cannot be automated and depends on subjective criteria and the experience of the analyst, its skill is demonstrated to be better than the other sensitivity estimates studied. Indeed, the manual subjective sensitivity estimate provides the best 60 km simulation of the cyclone.

These results raise questions about the advantages offered by adjoint methods in comparison to subjective estimations of IC sensitivity for real targeting campaigns. Although the simulations used in this study extend to 60 h, and no convective scheme is used in the adjoint run, the coarse resolution of the model grid (60 km) and the predominantly baroclinic character of the initial cyclogenesis event raised expectations that accurate results from the adjoint model could be obtained. Perhaps, an extension of the analysis including the adjoint of the data assimilation scheme to obtain sensitivities to observations, as in Langland and Baker (2004), would be informative about the role of the additional observations on the forecast. This analysis remains for future work, as the adjoint of the 3DVAR system used is not currently available. Even for a perfect adjoint model in ideal conditions of linear regime, however, Ancell and Hakim (2007a,b) suggest that targeting regions of largest adjoint sensitivity may be inferior to targeting other nearby areas where new observations can yield larger analysis increments in regions that still have large sensitivity. Yet the linear assumption underlying the adjoint model results remains the most likely source for adjoint-derived sensitivity inaccuracies in our experimental setup owing to the 60 h forecast length. Aiming to improve 60 h forecasts of intense Mediterranean cyclones is beyond the linear adjoint model capabilities owing to the important influence of non-linear processes, and future targeting campaigns in the region should restrict the use of adjoint methods to shorter forecast times and consider alternative methods, such as the herein called 'subjective'.

Regarding its application within future operational campaigns such as MEDEX Phase II, in a region such as the Western Mediterranean, where details about the low-level circulation and moisture distribution are crucial for an accurate forecast of heavy rainfall and damaging winds, operational adaptive observation strategies could provide large benefits for short-range forecasting out to 36–72 h. However, the results of this study raise questions about the optimal way to estimate the sensitivity of a given forecast aspect to the ICs fields, in order to utilize the adaptive observing platforms in an efficient manner. Results from inverting the order of the targeted soundings from the adjoint sensitivity estimation show that it would had been more valuable to take soundings in some regions with lower sensitivity than in regions with the highest adjoint-derived sensitivity. This discouraging result reduces our confidence in the adjoint method to provide useful guidance on where to deploy the limited resources usually available in real targeting campaigns with an operational set-up similar to our experimental framework.

Questions regarding whether these findings are representative of the most typical situations producing hazardous weather in the Western Mediterranean remain open and need to be addressed in the future. However, the complex and computationally expensive adjoint model is shown to be outdone by a human-generated subjective sensitivity estimate in an adaptive observation framework for this individual case of a classic western Mediterranean cyclogenesis event. Alternative methods that permit to assess the impact of a given set of extra observations on a forecast aspect, such as the sensitivity to observations or the ensemble transform Kalman filter techniques needs to be considered when planning future Mediterranean targeting campaigns.

9. Acknowledgments

We are grateful to C. Bishop, R. Errico and two anonymous reviewers for their comments and suggestions. This work was performed while the leading author held a National Research Council Research Associateship Award at the NOAA/National Severe Storms Laboratory. This research was mainly developed in the framework of the WMO-THORPEX ‘Mediterranean Experiment MEDEX’ and ENSEMBLE (CGL2005-05681/CLI, Spain) projects. Computer support provided by NCAR/Scientific Computer Division (which is sponsored by the National Science Foundation) for model data preprocessing is also acknowledged.

References

Ancell, B. and Hakim, G. J. 2007a. Comparing adjoint- and ensemble-sensitivity analysis with applications to observation targeting. *Mon. Wea. Rev.* **135**, 4117–4134.

Ancell, B. C. and Hakim, G. J. 2007b. Interpreting adjoint and ensemble sensitivity toward the development of optimal observation targeting strategies. *Meteorol. Z.* **16**, 635–642.

Badger, J. and Hoskins, B. 2001. Simple initial value problems and mechanisms for baroclinic growth. *J. Atmos. Sci.* **58**, 38–49.

Baker, N. L. and Daley, R. 2000. Observation and background adjoint sensitivity in the adaptive observation targeting problem. *Q. J. R. Meteorol. Soc.* **126**, 1431–1454.

Bao, J.-W. and Kuo, Y.-H. 1995. On-off switches in the adjoint method: step functions. *Mon. Wea. Rev.* **123**, 1589–1594.

Barker, D. M., Huang, W., Guo, Y. R., Bourgeois, A. and Xiao, Q. N. 2004. A three-dimensional variational data assimilation system for MM5: implementation and initial results. *Mon. Wea. Rev.* **132**, 897–914.

Benjamin, S. G. 1983. *Some Effects of Heating and Topography on the Regional Severe Storm Environment*. 265 pp. [Available from University Microfil, 300 N. Zeeb Rd., P.O. Box 1346, Ann Arbor, MI 46801-1346.], Ph.D. Thesis, The Pennsylvania State University.

Berliner, L. M., Lu, Z.-Q. and Snyder, C. 1999. Statistical design for adaptive weather observations. *J. Atmos. Sci.* **56**, 2536–2552.

Bishop, C., Etherton, B. and Majumdar, S. 2001. Adaptive sampling with the ensemble transform Kalman filter. Part I: theoretical aspects. *Mon. Wea. Rev.* **129**, 420–436.

Burpee, R. W., Marks, D. G. and Merrill, R. T. 1984. An assessment of Omega dropwindsonde data in track forecasts of Hurricane Debby (1982). *Bull. Amer. Meteor. Soc.* **65**, 1050–1058.

Carlson, T. N. 1991. *Mid-Latitude Weather Systems*. HarperCollins, London , 507 pp.

Daley, R. 1991. *Atmospheric Data Analysis*. Cambridge University Press, London , 457 pp.

Doerenbecher, A. and Bergot, T. 2001. Sensitivity to observations applied to fastex cases. *Nonlin. Proc. Geophys.* **8**, 467–481.

Dudhia, J. 1989. Numerical study of convection observed during the winter monsoon experiment using a mesoscale two-dimensional model. *J. Atmos. Sci.* **46**, 3077–3107.

Dudhia, J., Gill, D., Guo, Y.-R., Manning, K., Bourgeois, A. and co-authors. 2002. *PSU/NCAR Mesoscale Modeling System: Tutorial Class notes and User's Guide: MM5 Modeling System Version 3*. Available from NCAR. Boulder, USA .

Emanuel, K. A., Raymont, D., Betts, A., Bosart, L., Bretherton, C. and co-authors. 1995. Report of the first prospectus development team of the U.S. weather research program to NOAA and the NSF. *Bull. Amer. Meteor. Soc.* **76**, 1194–1208.

Errico, R. M. 1997. What is an adjoint model? *Bull. Amer. Meteor. Soc.* **78**, 2577–2591.

Errico, R. M. and Raeder, K. D. 1999. An examination of the accuracy of the linearization of a mesoscale model with moist physics. *Q. J. R. Meteorol. Soc.* **125**, 169–195.

Errico, R. M., Vukićević, T. and Raeder, K. 1993. Examination of the accuracy of a tangent linear model. *Tellus* **45A**, 462–477.

Fritsch, J., Hilliker, J., Ross, J. and Vislocky, R. 2000. Model consensus. *Wea. Forecast.* **15**, 571–582.

Gelaro, R., Buizza, R., Palmer, T. N. and Klinker, E. 1998. Sensitivity analysis of forecast errors and the construction of optimal perturbations using singular vectors. *J. Atmos. Sci.* **55**, 1012–1037.

Gelaro, R., Langland, R. H., Rohaly, G. D. and Rosmond, T. E. 1999. An assessment of singular-vector approach to targeted observing using the fastex dataset. *Q. J. R. Meteorol. Soc.* **125**, 3299–3327.

Gelaro, R., Reynolds, C. A., Langland, R. H. and Rohaly, G. D. 2000. A predictability study using geostationary satellite wind observations during NORPEX. *Mon. Wea. Rev.* **128**, 3789–3807.

Gilmour, I., Smith, L. A. and Buizza, R. 2001. Linear regime duration: is 24 hours a long time in synoptic weather forecasting? *J. Atmos. Sci.* **58**, 3525–3539.

Grell, G. A., Dudhia, J. and Stauffer, D. R. 1994. *A description of the fifth-generation Penn State/NCAR mesoscale model (MM5)*. NCAR Tech. Note NCAR/TN-398+STR.

Hakim, G. J. and Torn, R. D. 2008. *Sanders Symposium Monograph* Volume 55 of *Meteorological Monographs*, chap. Ensemble synoptic analysis. Amer. Meteor. Soc.

Homar, V., Ramis, C. and Alonso, S. 2002. A deep cyclone of african origin over the western mediterranean: diagnosis and numerical simulation. *Ann. Geophys.* **20**, 93–106.

Homar, V. and Stensrud, D. J. 2004. Sensitivities of an intense mediterranean cyclone: analysis and validation. *Q. J. R. Meteorol. Soc.* **130**, 2519–2540.

Hong, S. Y. and Pan, H. L. 1996. Nonlocal boundary layer vertical diffusion in a medium-range forecast model. *Mon. Wea. Rev.* **124**, 2322–2339.

Jansà, A., Genovés, A., Picornell, M. A., Campins, J., Riosalido, R. and co-authors. 2001. Western Mediterranean cyclones and heavy rain. *Meteorol. Appl.* **8**, 43–56.

Kain, J. S. 2002. The kain-fritsch convective parameterization: an update. *J. Appl. Meteorol.* **43**, 170–181.

Kain, J. S. and Fritsch, J. M. 1993. Convective parameterization for mesoscale models: the kain-fritsch scheme. In: *The Representation of Cumulus Convection in Numerical Models* (eds. K. A. Emanuel and D. J. Raymond). Amer. Meteor. Soc p. 246.

Langland, R. H. and Baker, N. L. 2004. Estimation of observation impact using the NRL atmospheric variational data assimilation adjoint system. *Tellus* **56A**, 189–201.

Langland, R. H., Elsberry, R. and Errico, R. M. 1995. Evaluation of physical processes in an idealized extratropical cyclone using adjoint sensitivity. *Q. J. R. Meteorol. Soc.* **121**, 1349–1386.

Langland, R. H., Gelaro, R., Rohaly, G. D. and Shapiro, M. 1999a. Targeted observations in fastex: adjoint-based targeting procedures and data impact experiments in iop17 and iop18. *Q. J. R. Meteorol. Soc.* **125**, 3241–3270.

Langland, R. H., Toth, Z., Gelaro, R., Szunyogh, I., Shapiro, M. and co-authors. 1999b. The north pacific experiment (NORPEX-98): targeted observations for improved north american weather forecasts. *Bull. Amer. Meteor. Soc.* **80**, 1363–1384.

Lewis, J. M., Raeder, K. D. and Errico, R. M. 2001. Vapor flux associated with return flow over the gulf of mexico: a sensitivity study using adjoint modeling. *Tellus* **53A**, 74–93.

Lord, S. J. 1996. The impact on synoptic-scale forecasts over the united states of dropwindsonde observations taken in the northeast pacific. In: *11th Conf. on Numerical Weather Prediction]*, Amer. Meteorol. Soc , Norfolk, VA, USA , 107–111.

Majumdar, S. J., Aberson, S. D., Bishop, C. H., Buizza, R., Peng, M. S. and co-authors. 2006. A comparison of adaptive observing guidance for atlantic tropical cyclones. *Mon. Wea. Rev.* **134**, 2354–2372.

Morss, R. E. and Emanuel, K. A. 2002. Influence of added observations on analysis and forecast errors: results from idealized systems. *Q. J. R. Meteorol. Soc.* **128**, 285–321.

Morss, R. E., Emanuel, K. A. and Snyder, C. 2001. Idealized adaptive observation strategies for improving numerical weather prediction. *J. Atmos. Sci.* **58**, 210–232.

Park, S. K. and Droegemeier, K. K. 1997. Validity of the tangent linear approximation in a moist convective cloud model. *Mon. Wea. Rev.* **125**, 3320–3340.

Pu, Z.-X., Kalnay, E., Sela, J. and Szunyogh, I. 1997. Sensitivity of forecast error to initial conditions with a quasi-inverse linear method. *Mon. Wea. Rev.* **125**, 2479–2503.

Ramis, C., Romero, R., Homar, V., Alonso, S. and Alarcón, M. 1998. Diagnosis and numerical simulation of a torrential precipitation event in Catalonia (Spain). *Meteorol. Atmos. Phys.* **69**, 1–21.

Reisner, J., Rasmussen, R. J. and Bruintjes, R. T. 1998. Explicit forecasting of supercooled liquid water in winter storms using the MM5 mesoscale model. *Q. J. R. Meteorol. Soc.* **124B**, 1071–1107.

Reynolds, C. A., Peng, M. S., Majumdar, S. J., Aberson, S. D., Bishop, C. H. and co-authors. 2007. Interpretation of adaptive observing guidance for atlantic tropical cyclones. *Mon. Wea. Rev.* **135**, 4006–4029.

Romero, R. 2001. Sensitivity of a heavy rain producing western mediterranean cyclone to embedded potential vorticity anomalies. *Q. J. R. Meteorol. Soc.* **127**, 2559–2597.

Sanders, F. and Gyakum, J. 1980. Synoptic-dynamic climatology of the "Bomb". *Mon. Wea. Rev.* **108**, 1589–1606.

Stein, U. and Alpert, P. 1993. Factor separation in numerical simulations. *J. Atmos. Sci.* **50**, 2107–2115.

Stensrud, D. J. and Fritsch, J. M. 1994. Mesoscale convective systems in weakly forced large-scale environments. Part III: numerical simulations and implications for operational forecasting. *Mon. Wea. Rev.* **122**, 2084–2104.

Szunyogh, I., Toth, Z., Emanuel, K. A., Bishop, C. H., Snyder, C. and co-authors. 1999. Ensemble-based targeting experiments during fastex: the effect of dropsonde data from the lear jet. *Q. J. R. Meteorol. Soc.* **125**, 3189–3217.

Toth, Z. and Kalnay, E. 1997. Ensemble forecasting at NCEP and the breeding method. *Mon. Wea. Rev.* **125**, 3297–3319.

Toth, Z., Szunyogh, I., Bishop, C., Majumdar, S., Morss, R. and co-authors. 2002. Adaptive observations at NCEP: past, present, and future. In: *Symposium on Observations, Data Assimilation, and Probabililstic Prediction*. Orlando, FL .

Truscott, B. and Richardson, D. 2003. *Atlantic THORPEX Observing System Test Project Plan*. EUCOS/SP/105.

Weissmann, M., Busen, R., Dörnbrack, A., Rahm, S. and Reitebuch, O. 2005. Targeted observations with an airborne wind lidar. *J. Atmos. Oceanic Technol* **22**(11), 1706–1719.

Xu, Q. 1996. Generalized adjoint for physical processes with parameterized discontinuities. Part I: basic issues and heuristic examples. *J. Atmos. Sci.* **53**, 1123–1142.

Zou, X., Huang, W. and Xiao, Q. 1998. *A User's Guide to the MM5 Adjoint Modeling System*. NCAR Tech. Note NCAR/TN-437+IA.

Zou, X., Vandenberghe, F., Pondeca, M. and Kuo, Y.-H. 1997. *Introduction to Adjoint Techniques and the MM5 Adjoint Modeling System*. NCAR Tech. Note NCAR/TN-435+IA.